Molecular Therapy
Methods & Clinical Development
Original Article

Micro-dystrophin gene therapy demonstrates long-term cardiac efficacy in a severe Duchenne muscular dystrophy model

Arden B. Piepho,[1] Jeovanna Lowe,[1] Laurel R. Cumby,[1] Lisa E. Dorn,[1] Dana M. Lake,[1] Neha Rastogi,[1] Megan D. Gertzen,[1] Sarah L. Sturgill,[1] Guy L. Odom,[2] Mark T. Ziolo,[1] Federica Accornero,[1] Jeffrey S. Chamberlain,[2] and Jill A. Rafael-Fortney[1]

[1]Department of Physiology & Cell Biology and Davis Heart and Lung Research Institute, College of Medicine, The Ohio State University, Columbus, OH, 43210, USA; [2]Department of Neurology and Sen. Paul D. Wellstone Muscular Dystrophy Specialized Research Center, University of Washington, Seattle, WA 98109, USA

Micro-dystrophin gene replacement therapies for Duchenne muscular dystrophy (DMD) are currently in clinical trials, but have not been thoroughly investigated for their efficacy on cardiomyopathy progression to heart failure. We previously validated Fiona/dystrophin-utrophin-deficient (dko) mice as a DMD cardiomyopathy model that progresses to reduced ejection fraction indicative of heart failure. Adeno-associated viral (AAV) vector delivery of an early generation micro-dystrophin prevented cardiac pathology and functional decline through 1 year of age in this new model. We now show that gene therapy using a micro-dystrophin optimized for skeletal muscle efficacy (AAV-μDys5), and which is currently in a clinical trial, is able to fully prevent cardiac pathology and cardiac strain abnormalities and maintain normal (>45%) ejection fraction through 18 months of age in Fiona/dko mice. Early treatment with AAV-μDys5 prevents inflammation and fibrosis in Fiona/dko hearts. Collagen in cardiac fibrotic scars becomes more tightly packed from 12 to 18 months in Fiona/dko mice, but the area of fibrosis containing tenascin C does not change. Increased tight collagen correlates with unexpected improvements in Fiona/dko whole-heart function that maintain impaired cardiac strain and strain rate. This study supports micro-dystrophin gene therapy as a promising intervention for preventing DMD cardiomyopathy progression.

INTRODUCTION

Duchenne muscular dystrophy (DMD) results from loss-of-function mutations in the gene encoding dystrophin located on the X chromosome. Dystrophin stabilizes striated muscle membranes by connecting the F-actin cytoskeleton to the extracellular matrix (ECM) through the dystrophin glycoprotein complex (DGC), thus distributing contractile forces.[1–3] Loss of dystrophin causes membrane damage upon muscle cell contraction, eventually leading to cell death. Fibrosis ultimately replaces damaged skeletal muscle and cardiac muscle, leading to loss of ambulation, respiratory insufficiency, and cardiomyopathy. Heart failure is currently the leading cause of death in males with DMD, and cardiomyopathy presents in up to 50% of female carriers.[4] Therefore, there is a growing need to identify better therapeutics to prevent DMD-associated cardiomyopathy.

Several gene therapy clinical trials are ongoing in young male patients with DMD using several versions of miniaturized "micro-dystrophin" (μDys) that can be packaged into an adeno-associated viral vector (AAV-μDys) with varied serotypes and regulatory cassettes to drive therapeutic expression. Although these micro-dystrophins have been comprehensively tested in skeletal muscles of animal models, studies were lacking in an animal model that displayed reduced whole-heart function, thereby preventing their thorough investigation for cardiac efficacy. Clinical heart outcomes will not be known for many years since cardiac function in patients only begins to decline in the late teens to early twenties, while treated patients were all between 5 and 14 years old.[2,5–7]

To evaluate preclinical cardiac efficacy of gene therapies and further understand DMD cardiac pathophysiology, a new dystrophic model that progresses to heart failure was recently generated. Fiona/dystrophin-utrophin-deficient ("Fiona/dko") mice have a rescued skeletal muscle pathology via transgenic human utrophin overexpression driven by the *ACTA1* promoter, while the heart remains a dystrophin-utrophin double-knockout tissue.[8] This model allows heart pathology to progress to contractile dysfunction indicative of heart failure (ejection fraction <45%) and parallels human DMD cardiomyopathy progression. Fiona/dko mice were previously validated, and administration of AAV6-CK8e-Hinge3-micro-dystrophin gene therapy at 4 weeks of age was able to prevent all functional and histological signs of cardiomyopathy through 12 months of age.[8] In the current study, we extend analysis of a new cohort of Fiona/dko mice to 18 months of age to evaluate cardiac efficacy of an updated version

Received 28 September 2022; accepted 3 February 2023;
https://doi.org/10.1016/j.omtm.2023.02.001.

Correspondence: Jill A. Rafael-Fortney, Department of Physiology & Cell Biology and Davis Heart and Lung Research Institute, College of Medicine, The Ohio State University, Columbus, OH, 43210, USA.
E-mail: rafael-fortney.1@osu.edu

Table 1. AAV-μDys5 dosages and percentages of Fiona/dko ventricular areas containing μDys-positive myocytes

Mouse number	Sex	Weight at injection (g)	Vector dosage (vg/kg)	μDys-positive myocyte (%) of ventricular area
3647	M	8.5	2.35×10^{14}	100
3666	F	8.5	2.35×10^{14}	100
3663	M	8.5	2.35×10^{14}	100
3548	F	15.1	1.33×10^{14}	99.7
3674	M	15.4	1.30×10^{14}	94.6
3551	F	13.0	1.54×10^{14}	100
3627	M	11.5	1.74×10^{14}	97.3

of micro-dystrophin gene therapy (AAV6-CK8e-μDys5) that is currently in clinical trials. The μDys5 construct is novel from that in our previous study as it contains a neuronal nitric oxide synthase (nNOS) binding site.[9] Dystrophin protein normally localizes nNOS to skeletal muscle membranes, and this construct is the only one of the three μDys constructs currently in clinical trials that contains this binding site.[10] However, nNOS is not normally co-localized to cardiomyocyte membranes with dystrophin and represents only a minor form of NOS in heart compared with endothelial and inducible NOS (eNOS and iNOS). In this study, we test whether AAV6-CK8e-μDys5 (μDys5) demonstrates continued efficacy for dystrophic cardiomyopathy.

RESULTS

μDys5 maintains normal cardiac function through 18 months of age

Fiona/dko mice were treated intravenously at 4 weeks of age with 2×10^{12} vector genomes of AAV6-CK8e-μDys5 (Table 1) or were left untreated. To determine the effect of μDys5 on overall heart function, blinded echocardiography was performed starting at 6 months of age and every 3 months until the planned endpoint at 18 months of age. Similar to the previous study, untreated Fiona/dko mice had significantly reduced ejection fractions (EFs) with a mean of 44% at both 6 and 9 months of age ($p = 0.0048$ and 0.0035, respectively, Welch's unpaired t test) and fractional shortening (FS) with a mean of 22% at both 6 and 9 months of age ($p = 0.0029$ and 0.0021, respectively, Welch's unpaired t test) compared with μDys5-treated Fiona/dko mice that maintained normal EFs of 61% and FS of 32% at both ages (Figures 1A and 1B). μDys5-treated mice maintained an EF above 55% and FS above 27% from 6 through 18 months of age, demonstrating long-term efficacy of the gene therapy on maintaining whole-heart pump function. Compared with μDys5 treated Fiona/dko mice, untreated Fiona/dko mice also had significantly lower width of intraventricular septum during systole (IVS,s) and trended toward increased left ventricular internal diameter during systole (LVID,s) at 6, 9, and 12 months of age, indicating dilated cardiomyopathy similar to patients with DMD (Figures 1C and 1D). Other measured parameters, including heart weight, were not different between treated and untreated mice, and males and females within each group were not different (Table S1; Figure S1).

Surprisingly, all whole-heart contractile function measurements in the untreated Fiona/dko mice at 15 and 18 months of age increasingly trended toward normal values and were no longer significantly different from the μDys5-treated mice. Since our previous study did not extend beyond the 12 month time point, we had not observed this effect. Since myocardial strain and strain rate are the first detectable cardiac abnormalities in patients with DMD that precede reductions in EF and even precede cardiac damage and fibrosis by up to several years,[11] we then assessed whether these indicators of cardiac muscle weakness are also normalized in Fiona/dko hearts. We performed speckle tracking echocardiography at 18 months of age, prior to euthanasia, to compare myocardial strain between the 2 groups. Interestingly, several strain and strain rate measurements, both systolic and diastolic, were still significantly abnormal in the 18-month-old untreated Fiona/dko mice compared with the μDys5-treated mice (Figures 1E–1G). Speckle tracking analysis of μDys5-treated mice revealed a significantly greater magnitude of circumferential strain and strain rates compared with untreated mice, thus indicating rescued cardiac muscle contractility in AAV-μDys5-treated mice (Figures 1E and 1F). AAV-μDys5 treatment also corrected diastolic function, evident through a greater magnitude of reverse strain rates compared with untreated mice (Figure 1G). Short axis radial strain, strain rate, and reverse strain rate exhibited the same preservation of function as circumferential indices (Table S2). Thus, treatment of mice with AAV-μDys5 preserved systolic and diastolic function as well as contractility, supporting that cardiac muscle performance was rescued by treatment. These data support that cardiac muscle weakness is still present in aged Fiona/dko mice despite improvements in whole-heart contractile function and that μDys5 is also able to prevent strain rate abnormalities.

To investigate the mechanism underlying improvement of whole-heart contractile function in Fiona/dko mice, we next tested whether the human utrophin transgene became expressed in the hearts of Fiona/dko mice over the 18 month experiment. We previously validated that transgenic utrophin was only expressed in skeletal muscles and not in the heart up until 12 months of age.[8] Western blot analysis was used to investigate utrophin protein in the hearts of the untreated and μDys5-treated 18-month-old Fiona/dko mice compared with previously collected 3- and 12-month-old Fiona/dko and wild-type C57BL/10 (C57) mouse hearts (Figure 2A). Immunoblotting with an antibody that detects both human and mouse utrophin (MANCHO3), previously used to detect transgenic utrophin in Fiona/dko skeletal muscles,[8] revealed utrophin expression only in C57 hearts but not in 18 month treated hearts or untreated Fiona/dko hearts at any age (Figure 2A). These data support that transgenic utrophin is not expressed in hearts from the older animals and cannot account for increased whole heart function in untreated Fiona/dko mice.

To validate that μDys5 expression was maintained through the 18 month study, western blots and immunofluorescence staining were performed. Western blotting with an antibody (MANDYS1) that reacts with mouse and human dystrophin encoded by exons

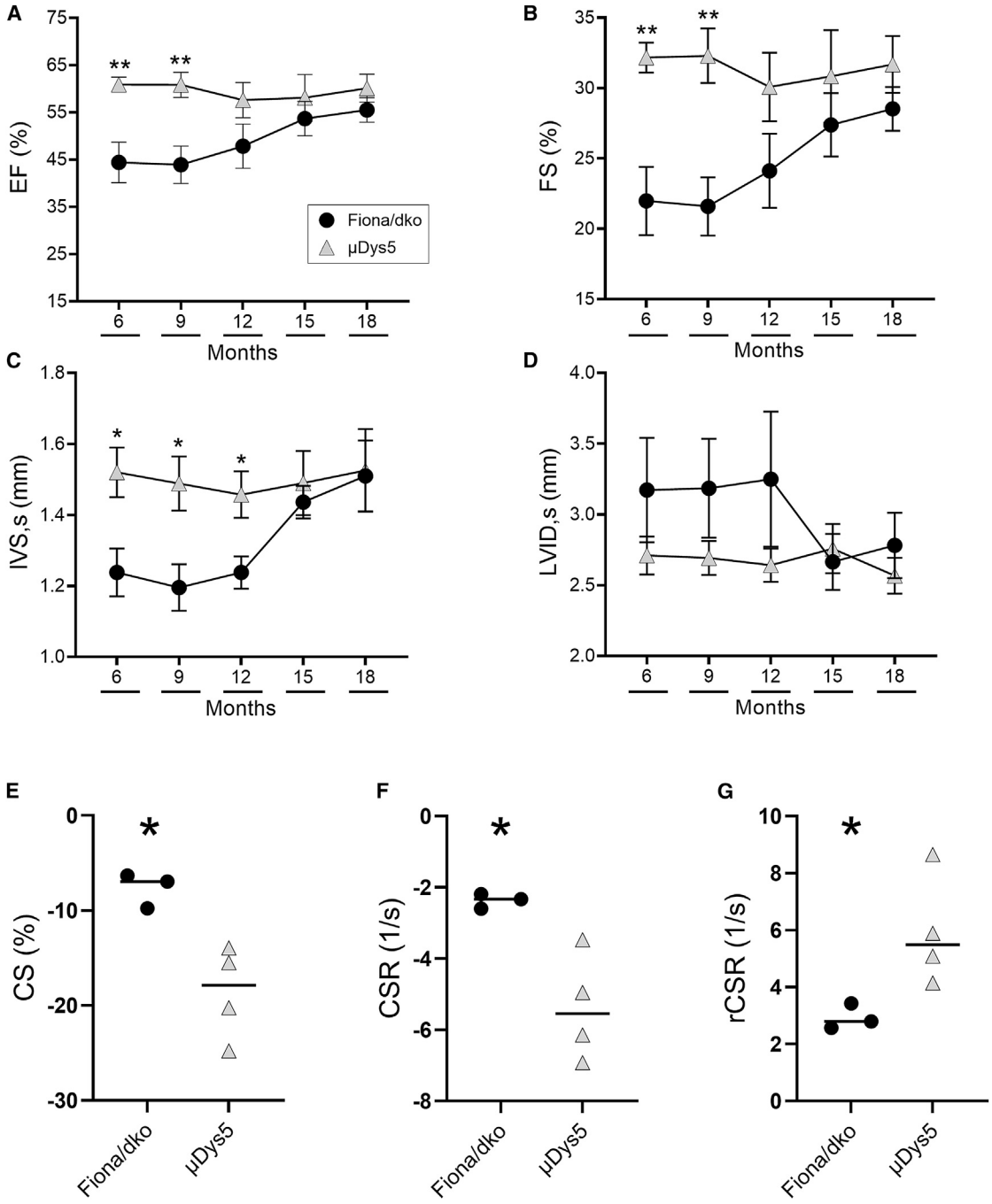

Figure 1. AAV6-μDys5 treatment prevents whole-heart dysfunction and myocardial strain abnormalities in Fiona/dko mice

(A–D) Longitudinal echocardiography at 6, 9, 12, 15, and 18 months of age in Fiona/dko and μDys5-treated Fiona/dko mice, showing (A) ejection fraction (EF), (B) fractional shortening (FS), (C) interventricular septal width, end systole (IVS,s), and (D) left ventricular internal diameter, end systole (LVID,s). Fiona/dko mice had significantly reduced function and structural remodeling at 6 and 9 months of age, which were prevented by treatment with AAV6-μDys5 at 4 weeks of age. Fiona/dko mouse heart function then improves beginning at 12 months of age through the 18 month endpoint. Heart rates were maintained at an average of 450 bpm throughout echocardiography. Welch's t test was performed for each parameter to compare groups at each time point (lines under x axes). Values are expressed as mean (markers) ± SEM (error bars). *$p \leq 0.05$, **$p \leq 0.01$. For (A)–(D): n = 4 males/5 females for Fiona/dko from 6 to 12 months, then n = 3 males/5 females from 15 to 18 months; n = 4 males/3 females for μDys5 group at all timepoints. (E–G) Circumferential strain rate analysis showed a significantly greater magnitude in μDys5-treated 18-month-old Fiona/dko mice compared with untreated mice, indicating improved strain and strain rate. Circumferential strain (CS) (E) and strain rate (CSR) (F) are measures of systolic function, while reverse peak strain rate (rCSR) (G) indicates diastolic function. AAV6-μDys5 gene therapy was effective for improving these functional parameters. Unpaired t test with Welch's correction for each measurement was performed. For (E)–(G): n = 3 (1 male [M], 2 females [2 Fs]) mice for Fiona/dko and n = 4 (2 Ms, 2 Fs) for μDys group. *$p \leq 0.05$.

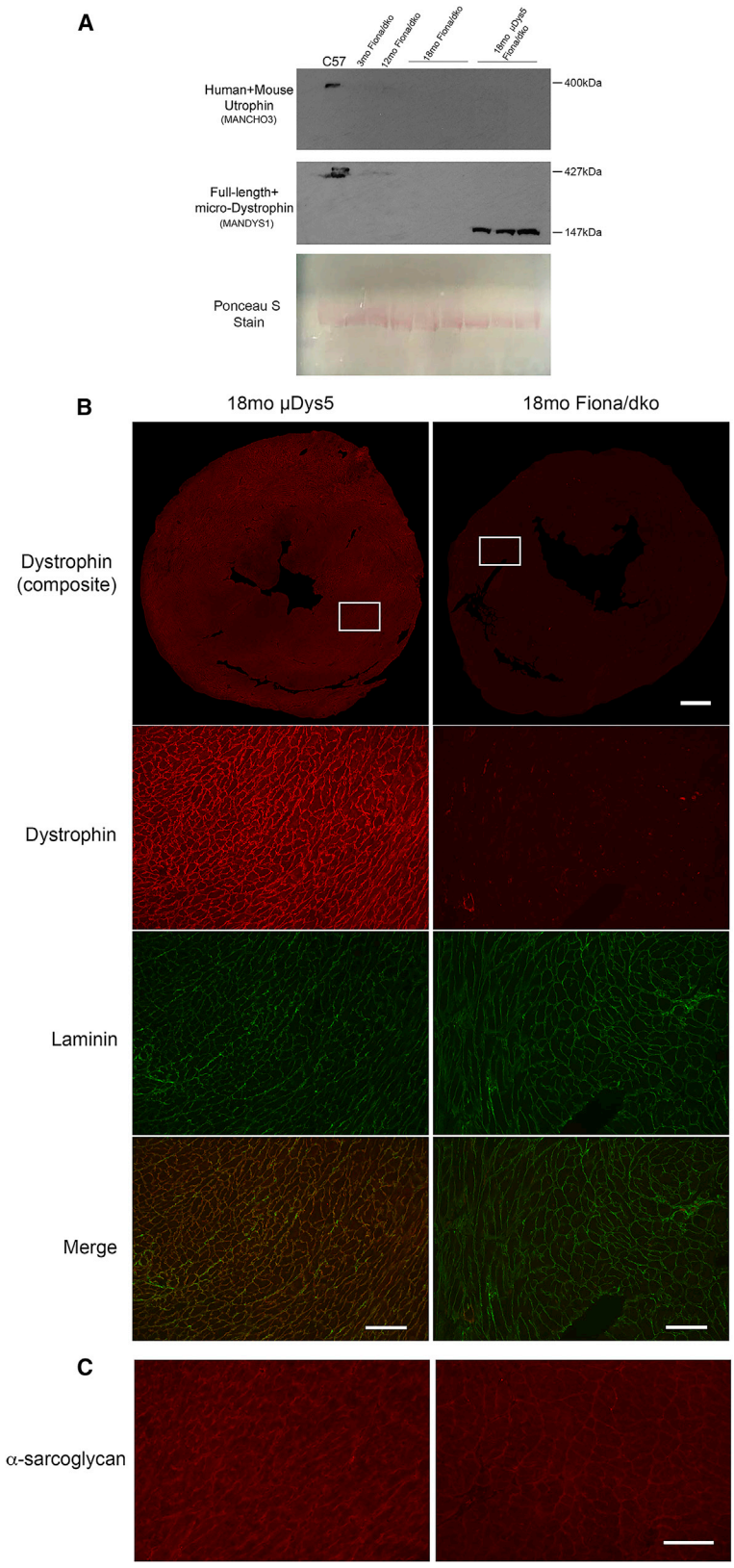

Figure 2. µDys5 protein is expressed and uniformly localized at cardiomyocyte membranes throughout Fiona/dko hearts at 18 months

(A) Western blot analysis of heart lysates from 3-, 12-, and 18-month-old Fiona/dko, 18-month-old µDys5 treated Fiona/dko, and C57BL/10 (C57) wild-type control mice. Blots were incubated with antibodies to detect both mouse and human utrophin (MANCHO3) (top) and dystrophin (MANDYS1) (bottom). Ponceau S staining shows equivalent loading between samples. Utrophin (MANCHO3) blot (top) shows that neither mouse nor human utrophin is present in any of the untreated or treated Fiona/dko hearts, validating complete knockout of mouse utrophin and that the "Fiona" human utrophin transgene does not become expressed in heart through 18 months of age. Dystrophin (MANDYS1) blot (bottom) shows that full-length dystrophin is present in C57 hearts and that micro-dystrophin is present only the µDys5-treated Fiona/dko mice. (B) Representative composites and zoomed immunofluorescence images of heart ventricular sections from treated and untreated Fiona/dko mice stained with a polyclonal antibody that detects the amino terminus of both mouse and human dystrophin (red). Zoomed panels show areas within white boxes in composites of dystrophin staining (red), laminin staining (green), and merged images and demonstrate that µDys5 is expressed in all cardiomyocytes surrounded by a basal lamina. Technical duplicates of all treated and untreated 18-month-old Fiona/dko mice were immunostained. Immunofluorescence staining shows the presence of dystrophin in the µDys5-treated mice (quantification in Table 1), but the absence of dystrophin localization in Fiona/dko hearts, except for a rare revertant cardiomyocyte. (C) Representative images of treated and untreated Fiona/dko mice stained with a polyclonal antibody that detects α-sarcoglycan. Scale bars: 500 µm, composites, and 100 µm, zoomed images.

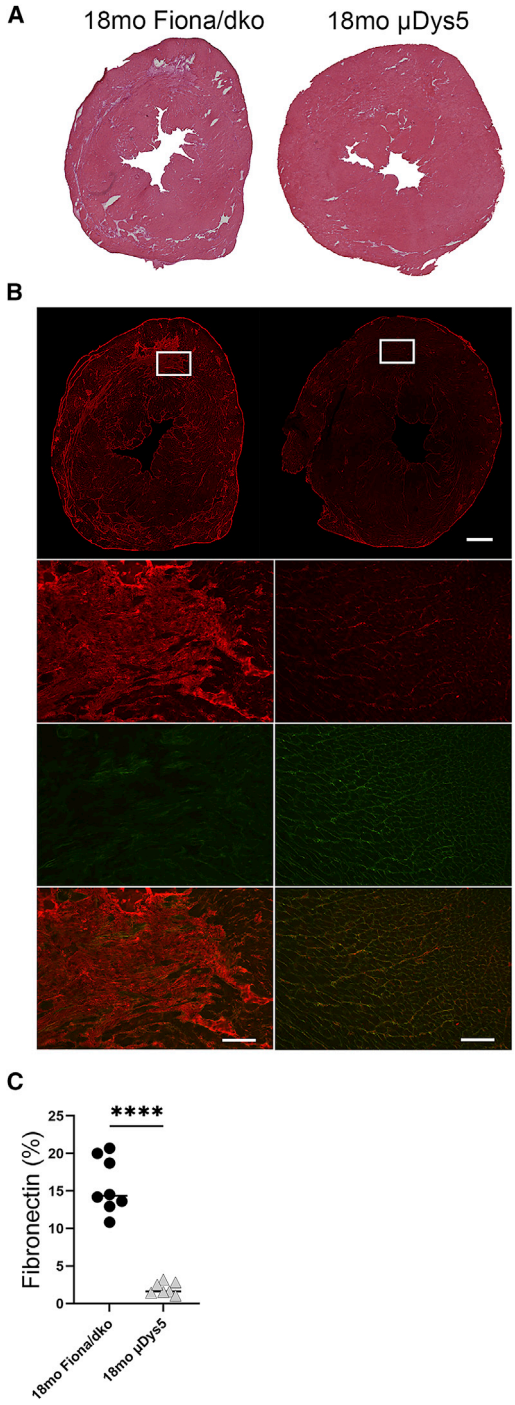

Figure 3. AAV6-µDys5 treatment prevents cardiac fibrosis in Fiona/dko mice

(A) Representative composite images of hematoxylin and eosin-stained transverse ventricular heart sections showing the complete prevention of histopathology in 18-month-old AAV-µDys5 (µDys5)-treated compared with untreated Fiona/dko mice. (B) Representative composite images of fibronectin immunofluorescence-stained (red) heart sections demonstrate absence of replacement fibrosis in µDys5 compared with Fiona/dko mice at 18 months of age. Zoomed images show areas within white boxes in composites of fibronectin (red) or co-staining with laminin (green) and merged images demonstrating fibrotic replacement in myocardium. Images shown are from samples near the mean for each group quantified in (C). (C) Quantification of fibrosis, shown as the percentage of area of ventricular composite sections containing fibronectin staining, demonstrates that µDys5 prevents fibrosis through 18 months of age compared with Fiona/dko hearts. Only small amounts of fibronectin normally surrounding vessels contributed to the quantification in µDys5 hearts. Statistical analysis performed with unpaired t test with Welch's correction; ****$p < 0.0001$. Dot plots display total n analyzed for each group. Scale bars: 500 µm composites, and 100 µm, zoomed images.

31–32, contained within the µDys5 protein, detects full-length mouse dystrophin in C57 and also detects µDys only in treated Fiona/dko hearts (Figure 2A). We next determined the percentage of cardiac muscle that contained cardiomyocytes expressing µDys5 protein. We performed immunofluorescence staining using a polyclonal antibody against the amino-terminal domain of human and mouse dystrophin (Figure 2B). All of the 18-month-old µDys5-treated mice had over 94% of the ventricular cross-sectional area containing µDys-positive cardiomyocytes (Figure 2B; Table 1). No dystrophin localization was detected in the untreated Fiona/dko hearts except for rare revertant myocytes due to exon skipping from the *mdx* mutant allele (Figure 2B). µDys5 also restored normal localization of α-sarcoglycan, the only dystrophin-glycoprotein complex member mildly reduced in dystrophic hearts[2] (Figure 2C).

µDys5 prevents cardiac damage through 18 months of age

Histological staining with hematoxylin and eosin of hearts from untreated 18-month-old Fiona/dko mice demonstrated large areas of fibrotic scarring within the myocardium (Figure 3A), similar to that previously observed in 12-month-old Fiona/dko mice.[8] These data suggest that functional improvement is not due to an absence of cardiac damage in these mice at 18 months. µDys5 treatment was able to prevent any accumulation of observable cardiac damage (Figure 3A).

To further investigate why whole-heart function may be improving in Fiona/dko mice after 1 year of age, we performed immunostaining for fibrosis-associated proteins to determine if the composition of cardiac scars was changing over time. Quantification of ventricular areas stained for fibronectin and tenascin C revealed an absence of fibrosis in µDys5-treated compared with untreated 18-month-old Fiona/dko hearts ($p < 0.0001$ for both) (Figures 3B, 3C, 4A, and 4C). However, there was no significant difference in tenascin C localization between untreated Fiona/dko mice at 12 and 18 months of age. Thus, the composition of this component of the fibrotic scars in untreated Fiona/dko hearts was not different with age and likely not contributing to observed improvements in function.

We next assessed the levels and packing of collagen via picrosirius red staining. This assay revealed a significant difference in collagen packing between 12- and 18-month-old Fiona/dko hearts (Figures 4B and 4D–4G). When imaged under polarized light, more tightly packed collagen appears as red birefringence, while more loosely packed collagen appears green. Hearts of 18-month-old untreated mice had

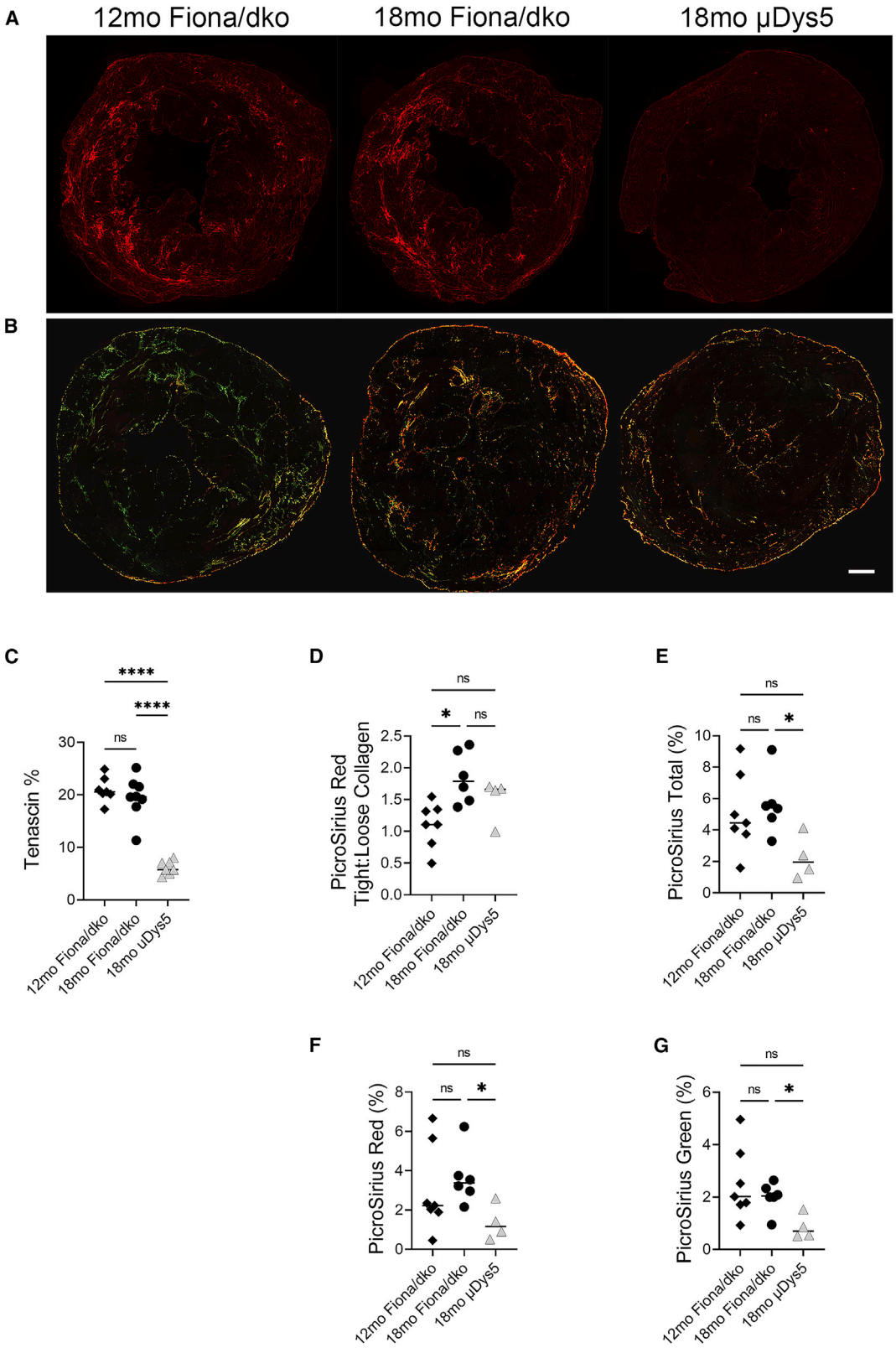

(legend on next page)

a higher ratio of red-to-green birefringence (1.8 red:green) and therefore more tightly packed collagen than the 12-month-old mice (1:1 red:green) ($p = 0.0166$, Dunnett's T3 multiple comparisons test) (Figure 4D). The total percentage of picrosirius red staining, red birefringence, and green birefringence were all significantly higher in the untreated 18-month-old Fiona/dko mice compared with μDys5-treated mice ($p = 0.0331$, 0.0374, and 0.0299, respectively, Dunnett's T3 multiple comparisons test) (Figures 4E–4G).

Since inflammation is chronically increased in Fiona/dko mice, we also stained for leukocytes in the hearts of treated and untreated mice to determine the effectiveness of μDys5 at preventing inflammation.[8] Colorimetric immuno-staining for CD45, a pan-leukocyte marker, demonstrated significantly reduced levels of ventricular areas containing immune cells in the hearts of 18-month-old μDys5-treated Fiona/dko mice (2.4%), representing normal localization of resident macrophages, compared with untreated Fiona/dko mice (5%), which include clusters of $CD45^+$ cells indicative of active inflammation ($p = 0.0003$, Welch's unpaired t test) (Figures 5A and 5B). Thus, μDys5 treatment was effective at preventing inflammatory infiltration at levels above resident leukocytes in the Fiona/dko hearts through 18 months of age.

DISCUSSION

Gene therapy trials for young male patients with DMD are currently underway, with 3 different constructs being tested. However, the efficacy of any constructs at preventing cardiomyopathy pathogenesis and heart failure progression has not been extensively studied. Since heart outcomes from human clinical trials will not be known for several years due to the long gap between treatment and onset of cardiomyopathy in the young boys in the trials, further preclinical testing in animal models of DMD cardiomyopathy is necessary. This study demonstrates that CK8e-μDys5, one of the transgenes being delivered in current clinical trials, is effective at preventing all assessed histological and functional heart abnormalities through 18 months of age in the Fiona/dko mouse model of isolated DMD cardiomyopathy.

Mice treated at 4 weeks of age with μDys5 were spared from cardiac pathology, including fibrosis and inflammation, and maintained normal heart function throughout the 18 month period. Surprisingly, untreated Fiona/dko mice in this study began to improve at 12 months of age and maintained improvement through 18 months of age in echocardiography parameters of whole-heart pump function, including EF and FS. However, speckle tracking echocardiography revealed strain abnormalities, both systolic and diastolic, in the untreated 18-month-old Fiona/dko mice compared with μDys5-treated mice. Strain and strain rate are likely indicators of cardiac muscle weakness.[12] We have previously reported dko cardiac muscles to generate less force compared with dystrophin-deficient *mdx* hearts and wild-type controls at very early stages of disease, months before whole-heart EF reductions.[13,14] We have also shown that strain rate abnormalities occur prior to reduced EF in dystrophic hearts, similar to that observed in patients with DMD.[15–18] Our previous studies measured strain and strain rate using magnetic resonance imaging (MRI). While MRI is a more sensitive measure, imaging takes approximately 1.5–2 h per mouse and costs upwards of $250 USD per imaging session. In the current study, we show that current ultrasound probes and software allow detection of strain abnormalities by echocardiography. Echocardiography imaging for these analyses takes only 15 min and is far less expensive. This study strongly suggests that both strain and whole-heart function should be measured to assess therapeutic interventions in DMD cardiomyopathy since they detect different abnormalities resulting from dystrophic cardiac muscle.

The underlying reason for increases in whole heart function in Fiona/dko mice is still unknown. However, utilizing polarized light imaging of Picrosirius red-stained Fiona/dko hearts enabled detection of differences in collagen type/cross-linking from 12 to 18 months of age. The older mice had a higher ratio of thicker and stiffer type I collagen compared with the more compliant and thinner type III collagen that was present at a higher ratio in younger mice.[19] The thicker type I collagen is associated with stiffening of the myocardium, so an increase in this collagen could be a compensatory mechanism as the mice age.[19] Whether this increase in tightly packed collagen compared with loosely packed collagen contributes to improvement in function after 12 months of age will require further testing but may partially contribute to the unexpected observation. However, this change is unlikely to account for the entire explanation.

Figure 4. AAV6-μDys5 treatment prevents tenascin C and collagen accumulation, but collagen packing changes with age in Fiona/dko mice

(A) Representative composite images of tenascin C immunofluorescence-stained heart sections demonstrate prevention of tenascin localization in μDys5 compared with Fiona/dko mice at 18 months of age and no change with age between 12- and 18-month-old Fiona/dko hearts. Images shown are from samples near the mean for each group quantified in (C). (B) Polarized images of Picrosirius red-stained heart sections show a difference in collagen packing in 12- compared with 18-month-old untreated and treated Fiona/dko mice as well as an overall decrease in collagen amount in μDys5-treated compared with untreated Fiona/dko mice at 18 months. Images shown are from samples near the mean for each group quantified in (D). (C) Quantification of tenascin C shown as the percentage of area of ventricular composite sections containing staining (red) demonstrates that μDys5 prevents increased tenascin through 18 months of age compared with 12- and 18-month-old Fiona/dko hearts. Tenascin percentages were not significantly different between 12 and 18 months of age for untreated Fiona/dko mice. Dot plots display total n analyzed for each group. Statistical analysis performed with Welch's ANOVA, followed by Dunnett's multiple-comparison post hoc test; ****$p < 0.0001$. (D–G) Quantification of collagen packing determined by red or green birefringence of Picrosirius red staining under polarized light, showing the ratio of red:green (D) and the total percentage area of ventricular composite sections containing both red and green birefringence (E), either red (F) or green (G). These data demonstrate that collagen becomes more tightly packed from 12 to 18 months of age, which was not affected by μDys5 treatment. Total, red, and green percentages of Picrosirius red staining were decreased by μDys treatment due to overall reduced fibrosis. Dot plots display total n analyzed for each group at each age. Statistical analysis performed with Welch's ANOVA ($p = 0.0166$ in D, 0.0331 in E, 0.0374 in F, and 0.0299 in G) followed by Dunnett's multiple-comparison post hoc test; *$p \leq 0.05$. 12-month-old Fiona/dko histological sections were from mice with reduced EFs previously published.[8] Scale bar: 500 μm.

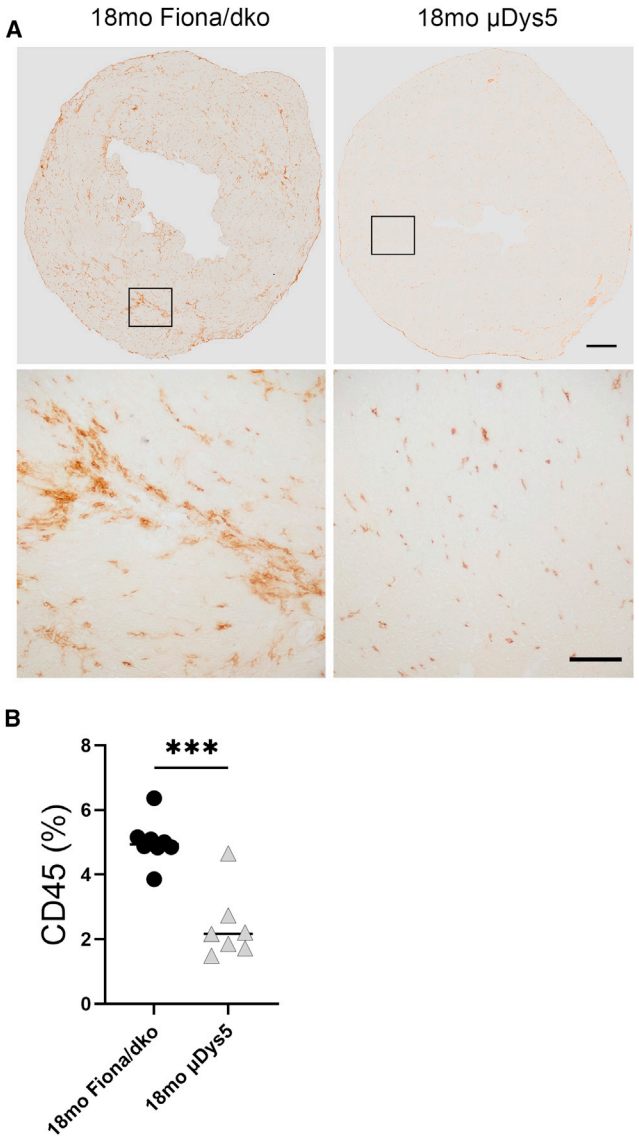

Figure 5. AAV6-µDys5 treatment prevents cardiac inflammation in Fiona/dko mice

(A) Representative composite (top) and zoomed (bottom) images of CD45 immunohistochemical staining (brown) of leukocytes in heart sections of 18-month-old untreated and µDys5-treated Fiona/dko mice. Zoomed images show areas within black boxes in composites. Images shown are from samples near the mean for each group quantified in (B) (untreated, F; µDys5 treated, M). (B) Quantification of inflammation shown as the percentage of area of ventricular composite sections containing CD45 pan-leukocyte staining demonstrates that µDys5 prevents inflammatory infiltrate through 18 months of age compared with untreated Fiona/dko hearts. Dot plots display total n analyzed for each group. Statistical analysis performed with unpaired t test with Welch's correction ($p = 0.0003$). ***$p \leq 0.01$. Scale bars: 100 µm.

Further testing will also be needed to determine if whole-heart pump function improvements occur in all aging Fiona/dko mice or if it was an artifact specifically driven in this cohort, which were raised during the start of the COVID-19 pandemic and were not handled or exposed to environmental stressors to the same extent as previously studied cohorts of mice. Although this reduced stress would likely not account for the functional improvements, it may account for the slightly less severe dysfunction at the earlier time points. Inflammation was still increased in untreated Fiona/dko hearts at 18 months of age, and therefore reduction of inflammation likely does not contribute to increased function. Future work is needed to determine how inflammation drives dystrophic cardiomyopathy progression. These studies will be vital for developing novel small-molecule or other adjunctive therapies since delivery of µDys gene therapy is unlikely to transduce all cardiomyocytes or possibly last throughout the human lifespan so will likely require synergistic treatments to ultimately optimize efficacy.

MATERIALS AND METHODS

Mice

To generate Fiona/dko (Fiona/Dmd^{mdx} $Utrn^{-/-}$) experimental mice[8] containing a full-length human utrophin cDNA under control of the Acta1 skeletal muscle-specific promoter (Tg (ACTA1-Utrn) 2^{Ked}) ("Fiona")[20] on a dko background, Fiona/Dmd^{mdx} $Utrn^{+/-}$ (Het/Fiona) mice were mated with Dmd^{mdx} $Utrn^{+/-}$ (Het) mice.[21] The Fiona transgene was detected by PCR with 5′-GTCAGGAGGGG CAAACCCGC-3′ (Utr_TG_For) and 5′-GTCGCTGCCCTTCTC GAGCC-3′ (Utr_TG_Rev) primers. The utrophin knockout allele was detected with 5′-GACAAACTGTCAGTTCTTAAG-3′ (UTRF1) and 5′-ACGAGACTAGTGAGACGTGC-3′ (NeoR), and the wild-type utrophin allele was detected with 5′-GTGAAGGATGT CATGAAAG-3′ (PU65) and 5′-TGAAGTCCGAAAGAGATACC-3′ (intron 7). Both mouse lines have been previously backcrossed for many generations over decades with C57BL/10-*mdx* mice.

AAV-µDys production and treatment study design

Fiona/dko mice at 4 weeks of age were randomly assigned to an untreated group (4 males [Ms], 5 females [Fs]) or a treated group (4 Ms, 3 Fs) receiving 2×10^{12} vector genomes of AAV6-CK8e-µDys5 in 100 µL total volume normal saline delivered via tail-vein injection. Design, generation, production, and titering of AAV6-CK8e-µDys5 was described previously.[9] We did not perform empty capsid treatments due to a lack of an observable effect in our prior experience, coupled with potential deleterious effects from excess cellular components that get packaged in the absence of vector genomes. µDys5-treated Fiona/dko, untreated Fiona/dko, and untreated littermate Het mice (3 Ms, 2 Fs) were enrolled to undergo longitudinal echocardiography at 6, 9, 12, 15, and 18 months and terminal histological analysis at 18 months of age. Echocardiography was started at 6 months since Fiona/dko mice were not different from Het controls in the previous study prior to that time point.[8] No treated Fiona/dko mice died during the course of this study. One untreated Fiona/dko mouse was found dead prior to the 15 month echocardiography time point. Het mice met IACUC-defined euthanasia criteria and were sacrificed before the 15 (n = 2) or 18 month (n = 3) endpoint due to large leg tumors and were therefore excluded from all terminal analyses, and their longitudinal data could not be completed, but

individual longitudinal echocardiography data up until euthanasia are included in Figure S2. After the final group of 18 month echocardiography measurements were completed, a subset of treated and untreated mice (n = 3 untreated [1 M, 2 Fs], n = 4 treated [2 Ms, 2 Fs]) were subjected to speckle tracking echocardiography to measure cardiac strain. A few days after the final echocardiography measurements, mice were euthanized by cervical dislocation, and striated muscles were harvested for biochemical and histological analysis. A portion of each tissue was flash frozen in liquid nitrogen, and another portion was embedded in optimal cutting temperature (OCT) medium (Sakura Finetek, 4583) as previously described.[16] Embedded tissues were used for histological analysis as described below. Mice, hearts, and spleens were weighed, and tibia length was measured during the dissection. Personnel who completed data collection and analysis were blinded to the genotypes and treatment of the animals throughout the study.

Western blot analysis

Heart tissue from treated and untreated Fiona/dko and C57BL/10 mice were homogenized and quantified using the *DC* Protein Assay (Bio-Rad, 5000166). 100 μg of each homogenate sample were separated using SDS-PAGE, transferred to nitrocellulose, reversibly stained with Ponceaus S, and then incubated with primary monoclonal antibody to dystrophin (MANDYS1(3B7), 1:100, exon31/32) or utrophin (MANCHO3, 1:100, cross-reacts with mouse and human utrophin) (University of Iowa Development Studies Hybridoma Bank). HRP-conjugated goat anti-mouse (1:5,000, Jackson ImmunoResearch Laboratories, 115035146) was used as the secondary antibody, and blots were developed with ECL Western Blotting Substrate (Thermo Fisher Scientific, 32106).

Histopathological analyses and quantification

OCT-embedded tissues were cryosectioned at 8 μm and then utilized for staining with hematoxylin and eosin, Picrosirius red, or antigen-specific antibodies. Primary antibodies included an affinity-purified rabbit polyclonal raised against the N terminus of mouse dystrophin that is dystrophin specific but cross-reacts with human dystrophin (1:100)[8]; rabbit polyclonal anti-human fibronectin (1:40, Abcam, 23750); rat monoclonal anti-mouse laminin-2 alpha 2 chain (1:500, Sigma-Aldrich, St. Louis, MO, USA, L0663); rabbit anti-mouse α-sarcoglycan antibody[22]; rabbit polyclonal anti-mouse and human tenascin C (1:100, Millipore Sigma, ab19011); and rat monoclonal anti-mouse CD45 (1:50, BD Pharmigen, 550539). Primary antibodies to dystrophin, α-sarcoglycan, fibronectin, and tenascin were detected with Alexa Fluor 555-conjugated goat anti-rabbit (1:200, Invitrogen, A-21429), laminin was detected with Cy3-conjugated goat anti-rat immunoglobulin G (IgG; 1:200, Jackson Immuno Research Laboratories, 112-165-167), and CD45 was detected with HRP-conjugated goat anti-rat antibody (1:200, Invitrogen, A10549) followed by development with ImmPact DAB peroxidase substrate (Vector, Burlingame, CA, USA, SK-4105). Transverse ventricular sections were imaged for quantification and analyzed using Adobe Photoshop CS6 as previously described.[23,24] Quantification of all histology was performed by individuals blinded to treatment. For fibronectin, tenascin C, and CD45, slides were imaged on a Nikon Eclipse 800 microscope under 10× or 20× objective using a Nikon DS-Ri2 digital camera driven by Nikon NIS-Elements Br software. For collagen analysis, sections were stained with a Picrosirius red staining kit (IHCWORLD, IW-3012) according to the manufacturer's recommendations.[23] The sections were imaged under a 10× objective with either bright field or polarized light for collagen packing quantification with a Zeiss Axioskop Widefield LM microscope and QImaging QCapture Pro software. For collagen and tenascin staining, 12-month-old Fiona/dko histological sections were from mice with reduced EFs previously published.[8]

Longitudinal echocardiography

Echocardiography was performed and analyzed by an investigator blinded to genotype and treatment in mice lightly anesthetized with 1.5% isoflurane. Measurements were taken using M-mode in the parasternal short-axis view at the level of the papillary muscles with a Vevo3100 FUJIFILM VisualSonics system and MX550D transducer as previously described.[8] Measurements were automatically calculated via the VevoLAB program as an average from at least 3 consecutive systole-diastole cycles.

Cardiac strain imaging and analysis

Echocardiography measurements were obtained using a FUJIFILM VisualSonics Vevo3100 MX550D transducer to observe parasternal short axis views, which were exported as 300 frame cine loops. Researchers were blinded to genotypes/treatments during echocardiography measurements and analysis. To perform speckle tracking analysis, tracking points were placed on the endocardial and epicardial borders of cine loops of parasternal short axis views using VevoStrain (v.3.1.1), which allowed for frame-by-frame tracking through the cardiac cycle for calculations of strain and strain rates. Short-axis speckle tracking analysis provides values of radial and circumferential movement, which differ based on the directionality of the vector of the tracking points. The software averages the data for each speckle along the left ventricular endocardial wall for strain and strain rate. Long-axis circumferential strain is also reported in Table S2.

Statistics

Quantitative data are displayed as individual data points or for longitudinal echocardiography as mean ± SEM. All statistical analyses were performed using Prism v.8.4.3 statistical software (GraphPad). Het mice met IACUC-defined euthanasia criteria and were sacrificed before the 15 (n = 2) or 18 (n = 3) month endpoint due to large leg tumors and were therefore excluded from all data analysis and are shown only as individual mice in Figure S2. The correct statistical test for each analysis was determined by first assessing the normality and variance of the data. For comparison between AAV-μDys5 treated and untreated Fiona/dko mice for fibronectin and CD45 staining and for strain measurements, Welch's t test was performed considering either equal or unequal variance as appropriate for each data analysis. For longitudinal echocardiography data, a

two-way ANOVA was performed to determine longitudinal changes in cardiac function (months of age), differences between groups, and their interaction effect. Since only group, but not months of age, showed a significant effect on parameters using this analysis, more detailed analysis was then carried out using Welch's t test between the 2 groups. A Welch's ANOVA followed by Dunnett's multiple-comparison post hoc test was used to compare tenascin C and all Picrosirius red staining quantification between the 3 groups. $p \leq 0.05$ was considered significant.

Study approval

Animal protocols were approved by the IACUC of The Ohio State University, in compliance with the NIH Guide for the Care and Use of Laboratory Animals (National Academies Press, 2011).

DATA AVAILABILITY

No genomics, proteomics, or structural data are included in this study, and no DNA sequences not previously published were used. The data supporting the studies presented in this manuscript can be found in the main text or the supplemental information. Additional information may be made available upon reasonable request to the corresponding authors as appropriate.

SUPPLEMENTAL INFORMATION

Supplemental information can be found online at https://doi.org/10.1016/j.omtm.2023.02.001.

ACKNOWLEDGMENTS

This work was supported by NIH R01 NS124681 and NIH P50 AR070604 Pilot Project (to J.A.R.-F.), NIH R01 AG060542 (to M.T.Z.), NIH T32 HL134616 (to A.B.P. and S.L.S.), NIH F30 HL145955 (to L.E.D.), and NIH P50 AR065139 (to J.S.C.).

AUTHOR CONTRIBUTIONS

A.B.P. coordinated terminal analyses, dissected mice, performed immuno- and histological staining and imaging, analyzed data, prepared the figures, and drafted the manuscript; J.L. performed tail-vein injections, coordinated longitudinal measurements, cut cryosections, and performed statistical analyses; L.E.D. performed blinded longitudinal echocardiography and analysis; L.R.C. maintained mouse colony and performed immunostaining for tenascin and fibronectin; D.M.L. performed blinded dystrophin staining and quantification; N.R. performed western blots; MDG genotyped and enrolled mice, and prepared AAV for injection; S.L.S. performed blinded strain echocardiography and analysis and drafted cardiac strain portions of the manuscript; G.L.O. prepared μDys vectors and edited the manuscript; M.T.Z. supervised and reviewed strain echocardiography data and edited the manuscript; F.A. supervised and reviewed longitudinal echocardiography data and edited the manuscript; J.S.C. designed and generated AAV-μDys and treatment strategy, reviewed final data, and edited the manuscript; J.A.R.-F. conceived, designed, and supervised the overall study, reviewed primary data and analysis, and drafted portions of the manuscript.

DECLARATION OF INTERESTS

J.S.C. is an inventor on various μDys patents, is a member of the scientific advisory board, and holds equity in Solid Biosciences.

REFERENCES

1. Guiraud, S., Aartsma-Rus, A., Vieira, N.M., Davies, K.E., van Ommen, G.J.B., and Kunkel, L.M. (2015). The pathogenesis and therapy of muscular dystrophies. Annu. Rev. Genom. Hum. Genet. *16*, 281–308.
2. Meyers, T.A., and Townsend, D. (2019). Cardiac pathophysiology and the future of cardiac therapies in Duchenne muscular dystrophy. Int. J. Mol. Sci. *20*, 4098. https://doi.org/10.3390/ijms20174098.
3. Townsend, D., Yasuda, S., McNally, E., and Metzger, J.M. (2011). Distinct pathophysiological mechanisms of cardiomyopathy in hearts lacking dystrophin or the sarcoglycan complex. Faseb. J. *25*, 3106–3114. https://doi.org/10.1096/fj.10-178913.
4. Mah, M.L., Cripe, L., Slawinski, M.K., Al-Zaidy, S.A., Camino, E., Lehman, K.J., Jackson, J.L., Iammarino, M., Miller, N., Mendell, J.R., and Hor, K.N. (2020). Duchenne and Becker muscular dystrophy carriers: evidence of cardiomyopathy by exercise and cardiac MRI testing. Int. J. Cardiol. *316*, 257–265. https://doi.org/10.1016/j.ijcard.2020.05.052.
5. Chamberlain, J.R., and Chamberlain, J.S. (2017). Progress toward gene therapy for Duchenne muscular dystrophy. Mol. Ther. *25*, 1125–1131.
6. Duan, D. (2018). Systemic AAV micro-dystrophin gene therapy for Duchenne muscular dystrophy. Mol. Ther. *26*, 2337–2356. https://doi.org/10.1016/j.ymthe.2018.07.011.
7. McNally, E.M., Kaltman, J.R., Benson, D.W., Canter, C.E., Cripe, L.H., Duan, D., Finder, J.D., Groh, W.J., Hoffman, E.P., Judge, D.P., et al. (2015). Contemporary cardiac issues in Duchenne muscular dystrophy working group of the national heart, lung, and blood institute in collaboration with parent Project muscular dystrophy. Circulation *131*, 1590–1598. https://doi.org/10.1161/circulationaha.114.015151.
8. Howard, Z.M., Dorn, L.E., Lowe, J., Gertzen, M.D., Ciccone, P., Rastogi, N., Odom, G.L., Accornero, F., Chamberlain, J.S., and Rafael-Fortney, J.A. (2021). Micro-dystrophin gene therapy prevents heart failure in an improved Duchenne muscular dystrophy cardiomyopathy mouse model. JCI Insight *6*, 146511. https://doi.org/10.1172/jci.insight.146511.
9. Ramos, J.N., Hollinger, K., Bengtsson, N.E., Allen, J.M., Hauschka, S.D., and Chamberlain, J.S. (2019). Development of novel micro-dystrophins with enhanced functionality. Mol. Ther. *27*, 623–635. https://doi.org/10.1016/j.ymthe.2019.01.002.
10. Crudele, J.M., and Chamberlain, J.S. (2019). AAV-based gene therapies for the muscular dystrophies. Hum. Mol. Genet. *28*. R102–r107. https://doi.org/10.1093/hmg/ddz128.
11. Ryan, T.D., Taylor, M.D., Mazur, W., Cripe, L.H., Pratt, J., King, E.C., Lao, K., Grenier, M.A., Jefferies, J.L., Benson, D.W., and Hor, K.N. (2013). Abnormal circumferential strain is present in young Duchenne muscular dystrophy patients. Pediatr. Cardiol. *34*, 1159–1165. https://doi.org/10.1007/s00246-012-0622-z.
12. Verhaert, D., Richards, K., Rafael-Fortney, J.A., and Raman, S.V. (2011). Cardiac involvement in patients with muscular dystrophies: magnetic resonance imaging phenotype and genotypic considerations. Circ. Cardiovasc. Imaging *4*, 67–76. https://doi.org/10.1161/CIRCIMAGING.110.960740.
13. Delfín, D.A., Xu, Y., Schill, K.E., Mays, T.A., Canan, B.D., Zang, K.E., Barnum, J.A., Janssen, P.M.L., and Rafael-Fortney, J.A. (2012). Sustaining cardiac claudin-5 levels prevents functional hallmarks of cardiomyopathy in a muscular dystrophy mouse model. Mol. Ther. *20*, 1378–1383. https://doi.org/10.1038/mt.2012.81.
14. Janssen, P.M.L., Hiranandani, N., Mays, T.A., and Rafael-Fortney, J.A. (2005). Utrophin deficiency worsens cardiac contractile dysfunction present in dystrophin-deficient mdx mice. Am. J. Physiol. Heart Circ. Physiol. *289*, H2373–H2378.
15. Lee, S., Lee, M., and Hor, K.N. (2021). The role of imaging in characterizing the cardiac natural history of Duchenne muscular dystrophy. Pediatr. Pulmonol. *56*, 766–781. https://doi.org/10.1002/ppul.25227.
16. Lowe, J., Floyd, K.T., Rastogi, N., Schultz, E.J., Chadwick, J.A., Swager, S.A., Zins, J.G., Kadakia, F.K., Smart, S., Gomez-Sanchez, E.P., et al. (2016). Similar efficacy from specific and non-specific mineralocorticoid receptor antagonist treatment of muscular dystrophy mice. J. Neuromuscul. Dis. *3*, 395–404.

17. Lowe, J., Kolkhof, P., Haupt, M.J., Peczkowski, K.K., Rastogi, N., Hauck, J.S., Kadakia, F.K., Zins, J.G., Ciccone, P.C., Smart, S., et al. (2020). Mineralocorticoid receptor antagonism by finerenone is sufficient to improve function in preclinical muscular dystrophy. ESC Heart Fail. *7*, 3983–3995. https://doi.org/10.1002/ehf2.12996.

18. Rafael-Fortney, J.A., Chimanji, N.S., Schill, K.E., Martin, C.D., Murray, J.D., Ganguly, R., Stangland, J.E., Tran, T., Xu, Y., Canan, B.D., et al. (2011). Early treatment with lisinopril and spironolactone preserves cardiac and skeletal muscle in Duchenne muscular dystrophy mice. Circulation *124*, 582–588. https://doi.org/10.1161/CIRCULATIONAHA.111.031716.

19. Frangogiannis, N.G. (2021). Cardiac fibrosis. Cardiovasc. Res. *117*, 1450–1488. https://doi.org/10.1093/cvr/cvaa324.

20. Tinsley, J., Deconinck, N., Fisher, R., Kahn, D., Phelps, S., Gillis, J.M., and Davies, K. (1998). Expression of full-length utrophin prevents muscular dystrophy in mdx mice. Nat. Med. *4*, 1441–1444.

21. Deconinck, A.E., Rafael, J.A., Skinner, J.A., Brown, S.C., Potter, A.C., Metzinger, L., Watt, D.J., Dickson, J.G., Tinsley, J.M., and Davies, K.E. (1997). Utrophin-dystrophin-deficient mice as a model for Duchenne muscular dystrophy. Cell *90*, 717–727.

22. Hainsey, T.A., Senapati, S., Kuhn, D.E., and Rafael, J.A. (2003). Cardiomyopathic features associated with muscular dystrophy are independent of dystrophin absence in cardiovasculature. Neuromuscul. Disord. *13*, 294–302.

23. Hauck, J.S., Lowe, J., Rastogi, N., McElhanon, K.E., Petrosino, J.M., Peczkowski, K.K., Chadwick, A.N., Zins, J.G., Accornero, F., Janssen, P.M.L., et al. (2019). Mineralocorticoid receptor antagonists improve membrane integrity independent of muscle force in muscular dystrophy. Hum. Mol. Genet. *28*, 2030–2045. https://doi.org/10.1093/hmg/ddz039.

24. Lowe, J., Kadakia, F.K., Zins, J.G., Haupt, M., Peczkowski, K.K., Rastogi, N., Floyd, K.T., Gomez-Sanchez, E.P., Gomez-Sanchez, C.E., Elnakish, M.T., et al. (2018). Mineralocorticoid receptor antagonists in muscular dystrophy mice during aging and exercise. J. Neuromuscul. Dis. *5*, 295–306. https://doi.org/10.3233/jnd-180323.